2

Modelling

… in which linear models and modal analysis are outlined, followed by the presentation of three test systems and mechanical equivalents, that are used throughout the thesis.

Whereas setting up a linearized power system model earlier has been a tedious and demanding task, new digital simulators feature automatic functions for this and can export a complete matrix model of the entire system. This considerably improves the reliability of the linear model and at the same time allows the analyst to concentrate on the analysis itself. An important prerequisite is that the structure and the properties of the exported model are well known. This is the aim of section 2.1, which describes the linearized differential-algebraic matrix equation and its properties using the more common description based on ordinary differential equations as a comparison. The power of linear models is to a great extent due to the existence of modal analysis, which is outlined in section 2.2. A few techniques for model reduction are also mentioned there, as they rely on modal analysis and are very common. Three test power systems are shortly described in section 2.3. They represent three different levels of complexity and are used throughout the thesis to offer a quantitative dimension to the analytical treatment. Mechanical analogs to a local mode and an inter-area mode are presented in section 2.4. They will be used extensively in the following chapters.

2.1 The Modelling Procedure

Setting up a linearized power system model for control design purposes typically involves going through three to five of the following consecutive steps:

- selecting component models;
- merging component models into a usually nonlinear system model;
- forming a matrix equation through linearization;
- eliminating algebraic variables;
- forming transfer functions.

While this procedure is straightforward in principle, it could pose practical difficulties due to the amount of variables and parameters to administrate. This problem is, however, solved by modern software that is commercially available. Software for time simulation of power systems generally offers only a limited number of component representations, which facilitates the first step. Before running simulations, the nonlinear system of equations describing the entire power system is created. Some simulators, such as EUROSTAG from Tractebel-Electricité de France [EUROSTAG], also feature functions for linearization and export of a linearized model of the entire power system. Fig. 2.1 shows the procedure for creating a linearized model.

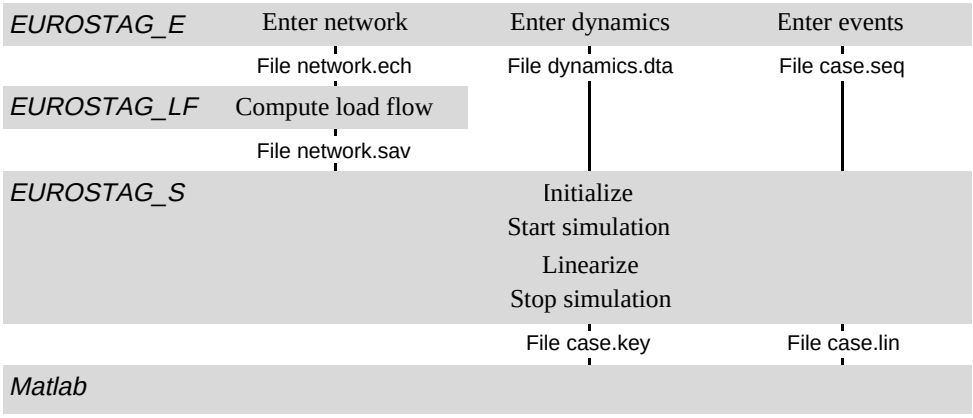

Fig. 2.1 A linearized model can be obtained from the time simulation program EUROSTAG: Network, dynamics and event files are created with the editor EUROSTAG_E. Having computed the initial load flow solution with EUROSTAG_LF, the simulator EUROSTAG_S is run. During steady state, the system is linearized and as simulation terminates two files containing the system model are written. These can then be read into e.g. Matlab.

The nonlinear time simulation model and the linearized model for control design thus contain the same initial models, use the same parameter set and operating point and are consequently guaranteed to be consistent. By finally loading the linearized system into for example Matlab [Matlab], transfer functions can conveniently be formed. In practice, the user thus only needs to select component models, connect them and enter their parameter values. To prove general properties through analytical reasoning, however, some modelling steps are outlined in more detail below.

Forming the Linear Differential-Algebraic Equation

The full system is in general described by a set of nonlinear vector valued *differential-algebraic equations* (DAE),

$$\begin{aligned} \dot{x}_d &= f(x_d, x_a, u) \\ 0 = e_a &= g(x_d, x_a, u) \\ y &= h(x_d, x_a, u) \end{aligned} \tag{2.1}$$

where x_d and x_a are the vectors of dynamic and algebraic variables respectively while u and y are the input and output vectors. The variables that are set to zero by the algebraic equation are denoted e_a. Alternatively u and y can be incorporated as algebraic variables together with x_a, forming a vector $\tilde{x}_a$. This gives a more compact description,

$$\begin{aligned} \dot{x}_d &= F(x_d, \tilde{x}_a) \\ 0 = e_a &= G(x_d, \tilde{x}_a) \end{aligned}$$

Small disturbance stability analysis treats only small deviations from a *stationary* operating point. A model linearized around this point is valid in its neighbourhood. Coordinates for small deviations from the linearization point (denoted by superscript 0) are then introduced,

$$\begin{aligned} \Delta x_d &= x_d - x_d^0 \\ \Delta x_a &= x_a - x_a^0 \\ \Delta u &= u - u^0 \\ \Delta y &= y - y^0 \end{aligned}$$

A *linear DAE* is then obtained by partial differentiation of the nonlinear functions *f*, *g* and *h*,

$$\begin{aligned} E_{dae} \frac{d}{dt} \begin{bmatrix} \Delta x_d \\ \Delta x_a \end{bmatrix} &= A_{dae} \begin{bmatrix} \Delta x_d \\ \Delta x_a \end{bmatrix} + B_{dae} \Delta u \\ \Delta y &= C_{dae} \begin{bmatrix} \Delta x_d \\ \Delta x_a \end{bmatrix} + D_{dae} \Delta u \end{aligned} \tag{2.2}$$

using

$$E_{dae} = \begin{bmatrix} I & 0 \\ 0 & 0 \end{bmatrix}$$

and the Jacobian matrices,

$$A_{dae} = \begin{bmatrix} A_{11} & A_{12} \\ A_{21} & A_{22} \end{bmatrix} = \begin{bmatrix} \frac{\partial f}{\partial x_d} & \frac{\partial f}{\partial x_a} \\ \frac{\partial g}{\partial x_d} & \frac{\partial g}{\partial x_a} \end{bmatrix} \qquad B_{dae} = \begin{bmatrix} B_1 \\ B_2 \end{bmatrix} = \begin{bmatrix} \frac{\partial f}{\partial u} \\ \frac{\partial g}{\partial u} \end{bmatrix}$$

$$C_{dae} = \begin{bmatrix} C_1 & C_2 \end{bmatrix} = \begin{bmatrix} \frac{\partial h}{\partial x_d} & \frac{\partial h}{\partial x_a} \end{bmatrix} \qquad D_{dae} = D_1 = \frac{\partial h}{\partial u}$$

An equivalent and very convenient expression is obtained by merging the dynamic states Δx_d and $\Delta \tilde{x}_a$ into a single vector Δx,

$$E\Delta\dot{x} = A\Delta x \tag{2.3}$$

where

$$\Delta x = \begin{bmatrix} \Delta x_d \\ \Delta \tilde{x}_a \end{bmatrix} = \begin{bmatrix} \Delta x_d \\ \Delta x_a \\ \Delta u \\ \Delta y \end{bmatrix}$$

Δx contains both dynamic states, algebraic variables, inputs and outputs. As shown in Fig. 2.1, EUROSTAG exports the linearized system as two files. One (case.lin) contains the matrices A and E, while the other (case.key) is a description of the contents of Δx. By inspecting E and A, inputs can be identified as independent algebraic variables. Similarly explicit outputs appear as variables upon which no other variables depend. Using this technique, the different parts of Δx are distinguished, E_{dae} is formed and A is partitioned into A_{dae}, B_{dae}, C_{dae} and D_{dae}.

While the general model of (2.1) could include time as an explicit variable, the linearized models of (2.2) and (2.3) are considered time invariant. Time varying properties such as changing operating points require repeated linearization. The fact that a valid linearized model is available gives access to the extensive set of techniques based on eigenanalysis. The most important features of this will be treated in Section 2.2.

In the following, Δ is omitted as all linear equations use variables that denote deviations from the linearization point.

Eliminating Algebraic Variables

In the following it is assumed that A_{22} is invertible. The algebraic variables can then be uniquely determined from the algebraic part of (2.2) as,

$$x_a = -A_{22}^{-1}\left(A_{21}x_d + B_2 u\right) \tag{2.4}$$

The elimination of x_a, yields a matrix *ordinary differential equation* (ODE),

$$\begin{aligned} \dot{x}_d &= A_{ode}x_d + B_{ode}u \\ y &= C_{ode}x_d + D_{ode}u \end{aligned} \tag{2.5}$$

where

$$\begin{aligned} A_{ode} &= A_{11} - A_{12}A_{22}^{-1}A_{21} \\ B_{ode} &= B_1 - A_{12}A_{22}^{-1}B_2 \\ C_{ode} &= C_1 - C_2A_{22}^{-1}A_{21} \\ D_{ode} &= D_1 - C_2A_{22}^{-1}B_2 \end{aligned}$$

Algebraic variables are mostly introduced as they naturally appear in a certain model structure with certain parameters, which is retained in the DAE model. The part of this structure that is contained in the matrix A_{22}, is in general lost in the conversion to ODE model as A_{22} is inverted. Due to this loss of information, the conversion is not reversible.

Note that a nonzero D_{ode} gives rise to a direct dependence between an input and an output. Installing a controller with a direct term, such as a proportional controller, between these yields an algebraic loop that may complicate simulations. This situation arises if D_1 is nonzero, or if both the input and the output are algebraic variables causing B_2 and C_2 to be nonzero.

While both the ODE and DAE descriptions can be considered as *state space* representations, control design methods known as *state space methods* predominantly handle only ODE models.

Forming Transfer Functions

An alternative to the state space approach is frequency domain methods based on *transfer functions*. Starting out from an ODE model, the corresponding set of transfer functions is defined as,

$$\frac{Y(s)}{U(s)} = C_{ode}\left(sI - A_{ode}\right)^{-1}B_{ode} + D_{ode} \tag{2.6}$$

where s is the Laplace operator or complex frequency. Transfer functions are well suited for determining *transfer function zeroes*. An input signal having the frequency of a transfer function zero is blocked and will not affect the output. While being unique for SISO systems, the definition of transfer zeroes for multi-input-multi-output (MIMO) systems is less clear [Maciejowski 1989]. As a transfer function maps inputs to outputs, it is very convenient when a model is to be based on measurements rather than a known physical structure. This requires entirely different methods than those presented above. Transfer functions carry magnitude and phase information of a signal path as a function of frequency which is used when selecting the proper phase shift of a controller. Compared to an ODE model, a transfer function model contains even less information as all structural system information has been removed.

2.2 Modal analysis

In a linear system, the dynamics can be described as a collection of modes. A mode is characterized by its frequency and damping and the activity pattern of the system states. If the damping is low, which is the case for electro-mechanical modes or *swing modes* in power systems, they can be thought of as resonances. The mode concept is based on a change of coordinates by diagonalization. As in many engineering areas an adequate choice of coordinates can decouple complex relations. This is particularly true with modal coordinates, which offer a convenient simplification of the system while being valid for the full system.

The Matrix Ordinary Differential Equation

The ODE system matrix A_{ode} can normally be diagonalized by the square *right modal matrix* Φ,

$$\begin{aligned} \Phi^{-1} A_{ode} \Phi &= \Lambda \\ A_{ode} \Phi &= \Phi \Lambda \end{aligned} \tag{2.7}$$

The columns of Φ are the *right eigenvectors* Φ_i to A_{ode}, while the diagonal elements of the diagonal matrix Λ are the *eigenvalues* λ_i of A_{ode}.

Similarly the *left modal matrix* Ψ holds the *left eigenvectors* Ψ_i as rows and also diagonalizes A_{ode},

$$\begin{aligned} \Psi A_{ode} \Psi^{-1} &= \Lambda \\ \Psi A_{ode} &= \Lambda \Psi \end{aligned} \tag{2.8}$$

The definitions (2.7) and (2.8) allow scaling of the eigenvectors with any complex number. In order for the left and right eigenvectors to be consistent it is required that $\Psi_i\Phi_j=1$ for $i=j$ (and $\Psi_i\Phi_j=0$ for $i\neq j$). This is conveniently guaranteed by computing Ψ as the inverse of Φ. If there are eigenvalues at the origin, Φ can however not be inverted. Ψ_i and Φ_i corresponding to such an eigenvalue are orthogonal and their product is zero. In practice eigenvalues are unlikely to exactly equal zero. Instead they take a very small value, leading to an ill-conditioned matrix. The inverse of Φ can then be computed, but its validity depends on the numerical accuracy that is used. It is therefore necessary to verify that the product of associated left and right eigenvectors of interest is one.

Provided that Ψ and Φ are available, the ODE system can be transformed into modal coordinates z through a transformation,

$$x_d = \Phi z$$

$$\begin{cases} \Phi\dot{z} = A_{ode}\Phi z + B_{ode}u \\ y = C_{ode}\Phi z + D_{ode}u \end{cases}$$

$$\begin{cases} \dot{z} = \Phi^{-1}A_{ode}\Phi z + \Phi^{-1}B_{ode}u \\ y = C_{ode}\Phi z + D_{ode}u \end{cases}$$

$$\begin{cases} \dot{z} = \Lambda z + \Psi B_{ode}u \\ y = C_{ode}\Phi z + D_{ode}u \end{cases}$$

Note that the dynamics now are governed by *uncoupled* first order differential equations — the modes. As seen in the block diagram of Fig. 2.2, the input u_j affects the mode i through element (i,j) of the *mode controllability matrix* [Porter and Crossley 1972] ΨB_{ode}. Analogously mode j appears in the output y_i to an extent that is determined by element (i,j) of the *mode observability matrix* [Porter and Crossley 1972] $C_{ode}\Phi$.

It is of utmost importance to observe that these measures of controllability and observability are *quantitative.* This is in contrast to the qualitative answer – *yes* or *no* – obtained by checking the rank of the controllability and observability matrices as in [Åström and Wittenmark 1990]. Chapters 3 and 4 will treat mode controllability and mode observability more in detail.

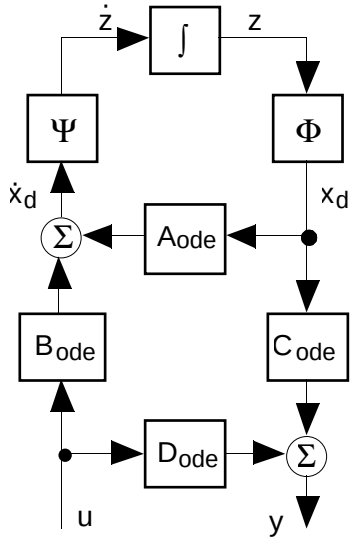

Fig. 2.2 Block diagram of a ODE matrix model showing dependence between mode coordinates *z*, dynamic states x_d, inputs *u* and outputs *y*.

Whereas the mode controllability and mode observability relate inputs and outputs to the mode, it may also be interesting to quantify how important a dynamic state is to the mode. This is conveniently done by computing the participation factors [Pérez-Arriaga 1982] from the left and right eigenvectors as,

$$p_{ki} = \Psi_{ik} \Phi_{ki}$$

The participation factor p_{ki} is dimensionless and gives a relative measure of how much element *k* in x_d participates in mode *i*.

With zero input the free motion of mode *i* depends only on its eigenvalue $\lambda_i=\sigma_i+j\omega_i$ and its initial value $z_i(0)$,

$$z_i(t) = z_i(0)e^{\lambda_i t} = z_i(0)e^{\sigma_i t}e^{j\omega_i t}$$

For electro-mechanical power system dynamics, the motion is typically oscillatory with frequency specified by ω while the oscillation envelope has a time constant equal to $1/|\sigma|$, where $-\sigma$ is the *absolute damping*. Improving damping of a mode is thus a matter of making its σ as negative as possible. The free motion may also be described using the initial value of x_d,

$$z_i(t) = \Psi_i x_d(0)e^{\lambda_i t}$$

It is obvious that the left eigenvector Ψ_i determines how much mode *i* is excited by $x_d(0)$. Mode *i* contributes with the following motion to the states $x_d(t)$,

$$\Phi_i z_i(0) e^{\lambda_i t} \tag{2.9}$$

The right eigenvector Φ_i thus gives a measure of how well mode *i* is coupled to each state. Note that the motions of all modes are summed for each state.

Introducing output feedback with the simple control law $u=Ky$ modifies the system dynamics. A nonzero direct matrix D_{ode} gives an algebraic loop, that may complicate simulations but is easy to solve,

$$u = \left(I - KD_{ode}\right)^{-1} KC_{ode} x_d$$

In modal coordinates, the new system description is,

$$\dot{z} = \left[\Lambda + \psi B_{ode}\left(I - KD_{ode}\right)^{-1} KC_{ode}\Phi\right] z \tag{2.10}$$

By instead eliminating *u*, a different but equivalent expression results,

$$\dot{z} = \left[\Lambda + \psi B_{ode} K\left(I - D_{ode}K\right)^{-1} C_{ode}\Phi\right] z$$

The equivalency is based on the equation,

$$\left(I - KD_{ode}\right)^{-1} K = K\left(I - D_{ode}K\right)^{-1}$$

that is proved by multiplying from the left with $I\text{-}KD_{ode}$ and from the right with $I\text{-}D_{ode}K$.

From (2.10) the sensitivity of eigenvalue *i* to changes in the scalar gain *K* can be obtained. For *small* gains (or if D_{ode} is zero) $I\text{-}KD_{ode}\approx I$, which gives,

$$\frac{\partial \lambda_i}{\partial K} = \Psi_i B_{ode} C_{ode} \Phi_i \tag{2.11}$$

For a single input single output (*SISO*) system B_{ode} and C_{ode} are column and row matrices respectively. As the resulting number is complex it gives both direction and magnitude of the movement for small values of *K*. This is in full accordance with the comments on the modal controllability and observability matrices above.

There are methods to determine more qualitatively which parameter affects what eigenvalue [Reinschke 1994]. These techniques set up matrices that indicate if the mode controllability and observability matrices are zero or not. As power systems are connected and there is no clear direction of cause and effect, exactly zero controllability or observability is very unlikely. Although being efficient, at least for reasonably small systems, such structural measures are therefore of little use for power systems control [von Löwis 1996].

The Linear Differential-Algebraic Equation

The modal matrices of a linear DAE are defined as in (2.12) and (2.13), starting out from the compact description of (2.3).

$$A\Phi_{dae} = E\Phi_{dae}\Lambda \tag{2.12}$$

$$\Psi_{dae}A = \Lambda\Psi_{dae}E \tag{2.13}$$

Partitioning the eigenvectors of (2.12) into a dynamic part and an algebraic part corresponding to x_d and $\tilde{x}_a$ clarifies the matrix dimensions

$$\begin{bmatrix} A_{11} & A_{12} \\ A_{21} & A_{22} \end{bmatrix} \begin{bmatrix} \Phi_{dae,d} \\ \Phi_{dae,a} \end{bmatrix} = \begin{bmatrix} I & 0 \\ 0 & 0 \end{bmatrix} \begin{bmatrix} \Phi_{dae,d} \\ \Phi_{dae,a} \end{bmatrix} \Lambda$$

Carrying through the multiplication and solving for $\Phi_{dae,a}$ yields,

$$\left(A_{11} - A_{12}A_{22}^{-1}A_{21}\right)\Phi_{dae,d} = \Phi_{dae,d}\Lambda$$

and

$$\Phi_{dae,a} = -A_{22}^{-1}A_{21}\Phi_{dae,d} \tag{2.14}$$

where the parenthesized expression is recognized as A_{ode}. It is now evident that the DAE description shares the eigenvalues and consequently the dynamic part of the eigenvectors with the ODE description. The algebraic part of the DAE eigenvectors can be obtained from the dynamic part by a simple transformation.

Similar expressions naturally apply for the left eigenvectors. Equation (2.13) can be rewritten as,

$$\begin{bmatrix} \Psi_{dae,d} & \Psi_{dae,a} \end{bmatrix} \begin{bmatrix} A_{11} & A_{12} \\ A_{21} & A_{22} \end{bmatrix} = \Lambda \begin{bmatrix} \Psi_{dae,d} & \Psi_{dae,a} \end{bmatrix} \begin{bmatrix} I & 0 \\ 0 & 0 \end{bmatrix}$$

which can be separated into,

$$\Psi_{dae,d}\left(A_{11}-A_{12}A_{22}^{-1}A_{21}\right)=\Lambda\Psi_{dae,d}$$

and

$$\Psi_{dae,a}=-\Psi_{dae,d}A_{12}A_{22}^{-1} \tag{2.15}$$

Fig. 2.3 illustrates the connections between different coordinates for a DAE system as compared to an ODE system. By tracing the arrows of the block diagram the same expressions as above can be obtained.

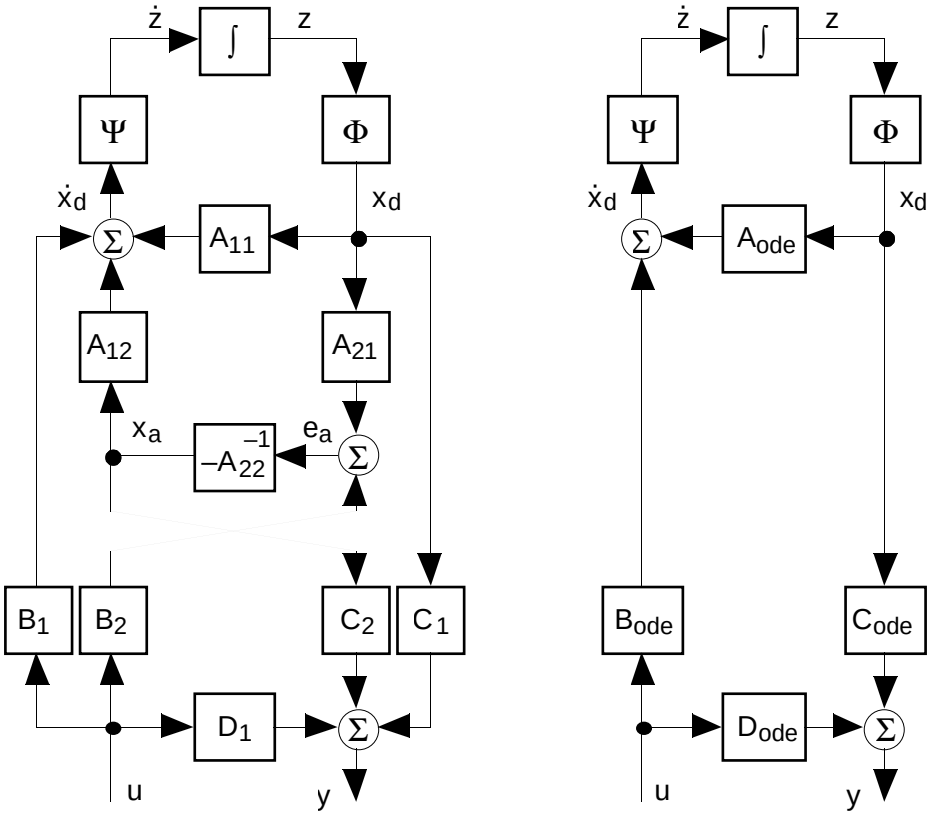

Fig. 2.3 Block diagram of a DAE (left) and an ODE matrix model (right) showing dependencies between mode coordinates z, dynamic states x_d, algebraic variables x_a, algebraic equation variables e_a, inputs u and outputs y.

$\Phi_{dae,d}$ and $\Psi_{dae,d}$ are equal to the ODE modal matrices Φ and Ψ and the corresponding eigenvectors have the same interpretation. The columns of $\Phi_{dae,a}$ show how the mode motions appear in the algebraic variables, while the rows of $\Psi_{dae,a}$ describe how the variables e_a, which summed up to zero in algebraic equations, affect the modes. Note that an algebraic equation may sum up current injections using voltage as algebraic variables, so that

element i of x_a and element i of e_a have different units. The corresponding eigenvector elements share the same property.

The expressions for the DAE eigenvectors given above are computationally efficient. The additional operations required to obtain the algebraic parts of the eigenvectors are not demanding. Routines that compute only selected eigenvalues and their eigenvectors are of course even more efficient. They are, however, less accessible and are for example not included in Matlab version 4.2. Matlab can, on the other hand, offer direct computation of the DAE eigenvectors, which may seem attractive. Entering the matrices A and E then gives the right eigenvectors, while use of their transpose yields the left eigenvectors since

$$\left(\Psi_{dae}A\right)^T = \left(\Lambda\Psi_{dae}E\right)^T$$
$$A^T\Psi_{dae}^T = E\Psi_{dae}^T\Lambda$$

The Matlab routine returns a diagonal matrix with eigenvalues and a matrix with right eigenvectors. The problem is that these matrices have the same size as A and E, which means that a number of the eigenvectors correspond to algebraic dynamics with infinite eigenvalues. The computation of these infinite eigenvalues and the associated eigenvectors increase the computation time considerably. Again the problem with scaling of the eigenvectors arises. To guarantee consistency the DAE eigenvectors should all be computed from Φ_i and Ψ_i (for which $\Psi_i\Phi_i$ =1) by using (2.14) and (2.15).

When the DAE system is transformed into modal coordinates, the input, output and modal matrices differ as compared to the ODE case. However the resulting modal controllability matrix $\Psi_{dae}B_{dae}$ and the modal observability matrix $C_{dae}\Phi_{dae}$ are the same.

The control law $u=Ky$ in a SISO DAE system changes the system dynamics: A_{dae} is replaced by $A_{dae}+B_{dae}KC_{dae}$. According to [Smed 1993] the sensitivity of mode i to a small gain K is,

$$\frac{\partial\lambda_i}{\partial K} = \frac{\Psi_{dae_i}\dfrac{\partial}{\partial K}\left(A_{dae}+B_{dae}KC_{dae}\right)\Phi_{dae_i} - \lambda_i\Psi_{dae_i}\dfrac{\partial E}{\partial K}\Phi_{dae_i}}{\Psi_{dae_i}E\Phi_{dae_i}}$$

where Ψ_{daei} and Φ_{daei} are the left and right DAE eigenvectors corresponding to mode i. If E contains only zeroes and ones, and if $\Psi_{daei}E\Phi_{daei}$ =1 the expression is substantially simplified,

$$\frac{\partial \lambda_i}{\partial K} = \Psi_{dae_i} B_{dae} C_{dae} \Phi_{dae_i} \tag{2.16}$$

Note that if each one of the input and output matrices contain only a single nonzero element being one, the eigenvalue sensitivity is obtained by simply multiplying one element of each of the right and left eigenvectors.

Model Reduction

As in all dynamic modelling, the purpose of the model should determine the complexity or resolution of the model. Highly simplified models are well suited for analytical treatment and intuitive understanding. The results obtained are then general and can easily be related to the included parameters, but their validity for the original system is limited. A model with full complexity would be more faithful but is in general too involved to be practically useful. In fact the term *full complexity* of a power system model is never used. Any power system model is instead a compromise between a good representation and a size that can be handled both regarding computational effort, setting of parameters and interpretation of results. An important technique to simplify a model, while maintaining its validity for a particular purpose is to remove dynamic states through *model reduction*. This is particularly useful in association with control design techniques such as H_∞ and LQG [Maciejowski 1989], that produce controllers whose complexity is related to that of the controlled system. To demonstrate the relationships between different model types, three examples of model reduction based on modal analysis are given here,

- time scale decomposition;
- modal equivalencing;
- transfer function residues.

If the network dynamics are included in a model for small disturbance stability analysis, they will show up as eigenvalues that are considerably faster than the electro-mechanical modes. Through *time scale decomposition* and a proper choice of coordinates the states may be partitioned in slow and fast ones, leading to,

$$\begin{bmatrix} I & 0 \\ 0 & \varepsilon \end{bmatrix} \frac{d}{dt} \begin{bmatrix} \Delta x_{slow} \\ \Delta x_{fast} \end{bmatrix} = A \begin{bmatrix} \Delta x_{slow} \\ \Delta x_{fast} \end{bmatrix} \tag{2.17}$$

which can be thought of as the result of improving the condition number of the system matrix. The elements of the diagonal matrix ε can be thought of as time constants and are small. By setting ε to zero (2.17) turns into the differential-algebraic equation (2.3). The fast states now algebraically

depend on the slow ones, and their eigenvalues and eigenvectors are eliminated. The reduction ignores the influence of ε on the eigenvalues of the slow states. In [Sauer et al 1987] expressions are given for how to take ε into account, so that the slow eigenvalues can be kept arbitrarily close to their original positions.

Although having reduced the model to contain only electro-mechanical modes, the number of states may still be too large. Then the eigenvectors can be used to formulate a simpler model that focuses only on the modes of interest, while omitting others. In damping studies the slowest *inter-area mode* is often of primary concern as it usually exhibits low damping. Its right eigenvector typically reveals that the system is split into two groups of machines, that swing against each other. Using this knowledge, the system can be reduced by modelling each machine group as an *equivalent machine*. The simplified system has two electro-mechanical modes; the inter-area mode and the *rigid body mode*, where the machine angles move in the same direction. Aggregating machines into groups that are modelled as equivalent machines is called *dynamic equivalencing*. *Coherent modal equivalencing* requires the machines within a group to swing exactly in phase with each other. [Ramaswamy et al 1995] briefly mentions coherence in order to explain *synchronic modal equivalencing*, where machines that swing in proportion to one or more reference machines may be algebraically represented.

The opposite of the inter-area mode is the *local mode*, in which a single machine or machine group swings against a large system. This practically does not excite the rigid body mode. A suitable model is then the *single machine infinite bus* system, where the large system is reduced into an infinite bus with constant frequency. This single mode system is the most widely used model for electro-mechanical power system dynamics and is one of the test systems of Section 2.3. As the structure is simple, analytical treatment is possible which will be made use of in the following. A nonlinear model can also be handled, which is shown in Chapter 5.

The equation for a transfer function of (2.6) requires all the eigenvalues of the system to be included in all transfer functions. This is mostly unnecessary, which is realized by expanding the transfer function in partial fractions as,

$$\frac{Y(s)}{U(s)} = G(s) = D_{ode} + \sum_{k=1}^{n} \frac{R_k}{s - \lambda_k}$$

where R_k is the *residue* of the $G(s)$ at the eigenvalue or pole λ_k. For a SISO system it is determined from input, output and modal matrices,

$$R_k = C_{ode}\Phi_k\Psi_k B_{ode}$$

The close relationship to the modal representation is obvious, as R_k can be said to quantify the participation of mode k in the dynamics as seen between the input and the output. The order of $G(s)$ may be reduced by omitting terms of the sum. This is done by sorting them by descending residues starting with the most *dominant poles* and truncating the series when the residues are considered negligibly small. Routines for determining the dominant pole spectrum are found in [Martins et al 1996].

2.3 Test Systems

Three test systems have been used. First a single mode system was chosen as it can be treated analytically. It can also demonstrate the influence of different control laws on one particular mode. Second a three machine system was selected as the least complex multi-mode system. It has a meshed network and thus represents the simplest nontrivial topology and is a complement to the longitudinal structure of the single mode system. The three machine system requires numerical computations as does the third test system which has twenty-three machines. It is a CIGRÉ model of the Swedish national power system, developed for comparing transient stability and voltage collapse performance of different simulators. Whereas the two first test systems are chosen for being manageable, the CIGRÉ model represents a realistic network topology with more detailed component models.

While the single mode system is manually modelled, the two others are modelled using EUROSTAG as described in Section 2.1. The resulting matrices of the DAE description contain the DAE matrix equations of the individual components and their controllers. For a system with k components, the matrices have the following structure:

$$\begin{bmatrix} E_1 & & & \\ & \ddots & & \\ & & E_k & \\ & & & 0 \end{bmatrix} \frac{d}{dt} \begin{bmatrix} x_1 \\ \vdots \\ x_k \\ v \end{bmatrix} = \begin{bmatrix} A_1 & & & B_1 \\ & \ddots & & \vdots \\ & & A_k & B_k \\ C_1 & \cdots & C_k & Y_{bus} \end{bmatrix} \begin{bmatrix} x_1 \\ \vdots \\ x_k \\ v \end{bmatrix}$$

While block matrices on the diagonal represent internal dynamics, the off-diagonal blocks specify the connections to other components, which are realised mainly through the network. The network and the passive loads are represented by algebraic equations for the current injection at each bus

using real and imaginary parts of the bus voltages *v* as algebraic variables. The lower right block matrix describing the network, equals the *differential bus admittance matrix*, Y_{bus}.

Single Machine Infinite Bus System

The single mode system is a standard example, found in textbooks like [Anderson and Fouad 1993] and [Kundur 1994]. It includes a synchronous generator connected to an infinite bus through a transformer and a transmission line circuit, illustrated by Fig. 2.4.

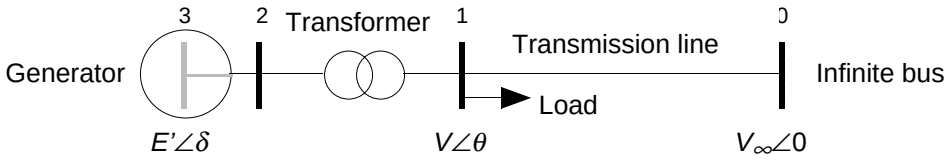

Fig. 2.4 One line diagram of single machine system.

For simplicity, all resistances are neglected and the generator is modelled as a constant voltage E' with phase angle δ behind the transient reactance X'_d. The system can be described by two differential equations for the machine and by algebraic equations for the power balance at the load bus,

$$\begin{aligned} \frac{2H}{\omega_R}\frac{d\omega}{dt} &= P_m - P_g \\ \frac{d\delta}{dt} &= \omega - \omega_R \\ P_{load} &= P_g + P_{tl} \\ Q_{load} &= Q_g + Q_{tl} \end{aligned} \tag{2.18}$$

H is the inertia constant of the machine in *MWs/MVA* and ω_R the nominal value of its electrical angular frequency ω in *rad/s*. P_m denotes the constant mechanical power with which the turbine drives the generator. P_g+jQ_g and P_{tl}+jQ_{tl} represent active and reactive power coming from the transformer and the transmission line into the load bus, where the load is P_{load}+jQ_{load}. The internal angle δ and the time derivative ω are given in *rad* and *rad/s* respectively. All other variables are normalized using *MVA* rating and rated bus voltage of the machine as base values.

Let X_t and X_{tl} be the series reactances of the transformer and the transmission line. If Y'_d and Y_{tl} represent $1/(X'_d+X_t)$ and $1/X_{tl}$ respectively, the power entering the load bus can be expressed as,

$$\begin{aligned} P_g &= Y_d' E' V \sin(\delta - \theta) \\ Q_g &= Y_d' E' V \cos(\delta - \theta) - Y_d' V^2 \\ P_{tl} &= -Y_{tl} V V_\infty \sin\theta \\ Q_{tl} &= Y_{tl} V V_\infty \cos\theta - Y_{tl} V^2 \end{aligned} \tag{2.19}$$

Introduce the state vector $[\omega\ \delta\ \theta\ V]^T$ and linearize. Assuming negligible variation in voltage magnitude the linearization gives,

$$\begin{bmatrix} M & 0 & 0 \\ 0 & 1 & 0 \\ 0 & 0 & 0 \end{bmatrix} \frac{d}{dt} \begin{bmatrix} \Delta\omega \\ \Delta\delta \\ \Delta\theta \end{bmatrix} = \begin{bmatrix} 0 & K_{\delta\delta} & K_{\delta\theta} \\ 1 & 0 & 0 \\ 0 & K_{\theta\delta} & K_{\theta\theta} \end{bmatrix} \begin{bmatrix} \Delta\omega \\ \Delta\delta \\ \Delta\theta \end{bmatrix} + \begin{bmatrix} 0 \\ 0 \\ -1 \end{bmatrix} P_{load} \tag{2.20}$$

with M and the synchronizing coefficients K defined as,

$$\begin{aligned} M &= \frac{2H}{\omega_R} \\ K_{\delta\delta} &= -Y'_d E' V \cos(\delta - \theta) = -K_{\delta\theta} = -K_{\theta\delta} \\ K_{\theta\theta} &= -Y'_d E' V \cos(\delta - \theta) - Y_{tl} V V_\infty \cos\theta \end{aligned} \tag{2.21}$$

System data for the single machine system are taken from the field test in Chapter 6 and are given in Appendix A.

The model of (2.20) can be generalized to the multi-machine case with an arbitrary network. The generator buses are then numbered 1..n, and the load buses are numbered n+1..n+m. The state vector is then expanded as,

$$\begin{bmatrix} \Delta\omega \\ \Delta\delta \\ \Delta\theta \end{bmatrix} = \begin{bmatrix} [\Delta\omega_1 \ \cdots \ \Delta\omega_n]^T \\ [\Delta\delta_1 \ \cdots \ \Delta\delta_n]^T \\ [\Delta\theta_{n+1} \ \cdots \ \Delta\theta_{n+m}]^T \end{bmatrix}$$

so that variables without subscript now denote vectors rather than scalars. The matrix equation is practically unaltered,

$$\begin{bmatrix} M & 0 & 0 \\ 0 & I & 0 \\ 0 & 0 & 0 \end{bmatrix} \frac{d}{dt} \begin{bmatrix} \Delta\omega \\ \Delta\delta \\ \Delta\theta \end{bmatrix} = \begin{bmatrix} 0 & K_{\delta\delta} & K_{\delta\theta} \\ I & 0 & 0 \\ 0 & K_{\theta\delta} & K_{\theta\theta} \end{bmatrix} \begin{bmatrix} \Delta\omega \\ \Delta\delta \\ \Delta\theta \end{bmatrix} + \begin{bmatrix} 0 \\ 0 \\ -I \end{bmatrix} P_{load} \tag{2.22}$$

where M is a diagonal matrix with $2H/\omega_R$ of each generator on the diagonal and P_{load} is an m-dimensional vector with the active power injection at

each load bus. An element in the matrices of synchronizing coefficients, $K_{\delta\theta}$ or $K_{\theta\delta}$ is now defined as,

$$K_{\delta\theta,ij} = Y_{i,j+n}E_i'V_{j+n}\cos\left(\delta_i - \theta_{j+n}\right) = K_{\theta\delta,ji} \tag{2.23a}$$

where Y_{ij} is element (i,j) of the bus admittance matrix, that specifies the admittance between buses i and j, that may be either internal generator buses or load buses. Similarly element (i,j) of $K_{\delta\delta}$ and $K_{\theta\theta}$ are defined as,

$$K_{\delta\delta,ij} = \begin{cases} Y_{ij}E_i'E_j'\cos\left(\delta_i - \delta_j\right) & i \neq j \\ -\sum_{\substack{j=1 \\ j\neq i}}^{n} K_{\delta\delta,ij} & i = j \end{cases} \tag{2.23b}$$

$$K_{\theta\theta,ij} = \begin{cases} Y_{i+n,j+n}V_{i+n}V_{j+n}\cos\left(\theta_{i+n} - \theta_{j+n}\right) & i \neq j \\ -\sum_{\substack{j=1 \\ j\neq i}}^{m} K_{\theta\theta,ij} & i = j \end{cases} \tag{2.23c}$$

Note that $K_{\delta\theta}$ is the transpose of $K_{\theta\delta}$ and that both $K_{\delta\delta}$ and $K_{\theta\theta}$ are symmetric. By applying (2.4) the load buses may be eliminated. This gives the ODE version of the system found in many textbooks.

Three Machine System

A three machine system has two oscillatory electro-mechanical modes and thus forms the first step towards a general multi-machine case. The nine bus system of [Anderson and Fouad 1993] is selected for having the generic meshed network with one mesh, see Fig. 2.5.

This system, also known as the WSCC 9 system, is commonly used in other studies such as for voltage stability [Arnborg 1997], and controller design [Chen et al 1995]. As both mode and network structure are uncomplicated, the results can easily be coupled to them. This makes the three machine system the basis for the development of control laws that can be applied in a general case.

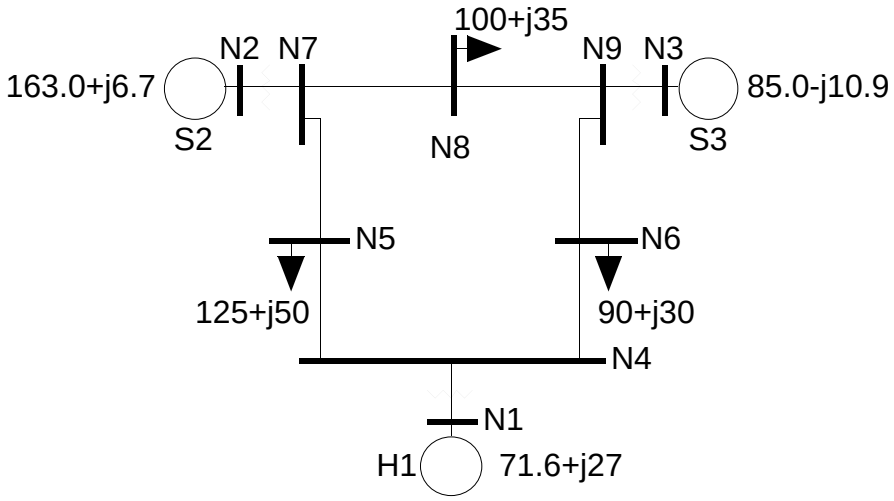

Fig. 2.5 Three machine system with generation and load in MVA.

A third order synchronous generator model is selected as this is the simplest machine model of EUROSTAG. It is sometimes referred to as the one-axis model, as it includes the direct axis but not the quadrature axis circuit. Damper windings are not included, and although saturation can be represented, this option is not used. The magnetization is controlled by a proportional AVR measuring terminal voltage. The mechanical input power is kept constant. One generator with AVR is described by eight state variables in the linearized DAE system model.

$$x_{gen} = \left[\lambda_f \;\; V_{ref} \;\; E_{FD} \;\; T_m \;\; \omega \;\; \delta \;\; I_q \;\; I_d\right]^T$$

The field flux linkage λ_f, the mechanical angular velocity ω and the machine angle δ are the dynamic states. (The machine angle is called *teta* in EUROSTAG.) AVR setpoint V_{ref}, field voltage E_{FD}, mechanical torque T_m, stator current along the d and q axis I_d and I_q are algebraic states. The structure of the DAE model of a generator with AVR and constant mechanical power is described by (2.24), where a dot denotes a non-zero matrix element. V_{busg} is the voltage at the generator terminals.

$$E_{gen}\frac{dx_{gen}}{dt} = A_{gen}x_{gen} + B_{gen}V_{busg}$$

$$diag\left(\begin{bmatrix}\bullet\\ \\ \\ \bullet\\ \bullet\end{bmatrix}\right)\frac{dx_{gen}}{dt} = \begin{bmatrix}\bullet & \bullet & & & & \bullet\\ & \bullet & & & & \\ & \bullet & \bullet & & & \\ & & & \bullet\ \bullet & & \\ \bullet & & \bullet & & \bullet\ \bullet & \\ & & & \bullet & & \\ & & & \bullet\ \bullet\ \bullet & & \\ & & & \bullet\ \bullet & & \bullet\end{bmatrix}x_{gen} + \begin{bmatrix}\ & \ \\ \bullet & \bullet\\ \ & \ \\ \ & \ \\ \ & \ \\ \ & \ \\ \bullet & \bullet\\ \bullet & \bullet\end{bmatrix}\begin{bmatrix}V_{busg,real}\\ V_{busg,imag}\end{bmatrix} \tag{2.24}$$

Both transformers and lines are modelled as series impedances but lines additionally have shunt admittances at each end. Loads are represented by impedances. Transformers, lines and loads can be modelled by expressing the current injections at each bus in the bus voltages. As the injections sum up to zero at each bus, the linearized network can be described as a matrix formulation of Kirchhoff's current law:

$$0 = I_{gen} - Y_{bus}V_{bus} \tag{2.25}$$

where Y_{bus} is the differential bus admittance matrix and I_{gen} holds the current injections of the generators.

In EUROSTAG, real and imaginary parts of the voltage at each bus enter the state vector as separate elements as in V_{busg} of (2.24). The full state vector holds the states of the controlled machines followed by the voltage variables. It thus contains 9 dynamic states and 33 algebraic states (5 per machine and 2 per network bus):

$$x^T = \left[x_{gen1}^T\ \ x_{gen2}^T\ \ x_{gen3}^T\ \ V_{bus1}^T\ \cdots\ V_{bus9}^T\right] \tag{2.26}$$

Using the state vector of (2.26), the full DAE system description is obtained by merging the descriptions of the network and all components,

$$E\frac{dx}{dt} = Ax$$

$$diag\left(\begin{bmatrix}E_{gen1}\\ E_{gen2}\\ E_{gen3}\\ 0\end{bmatrix}\right)\frac{dx}{dt} = \begin{bmatrix}A_{gen1} & & & B_{gen1}\\ & A_{gen2} & & B_{gen2}\\ & & A_{gen3} & B_{gen3}\\ C_{gen1} & C_{gen2} & C_{gen3} & Y_{bus}\end{bmatrix}x \tag{2.27}$$

Note that while A_{gen} and E_{gen} are unaltered from (2.24), B_{gen} is now related to the voltages at all buses, and C_{gen} represent the current injections of the machines. Referring to Fig. 2.5 for notation, a sparsity plot of the system matrix A of (2.27) is shown in Fig. 2.6.

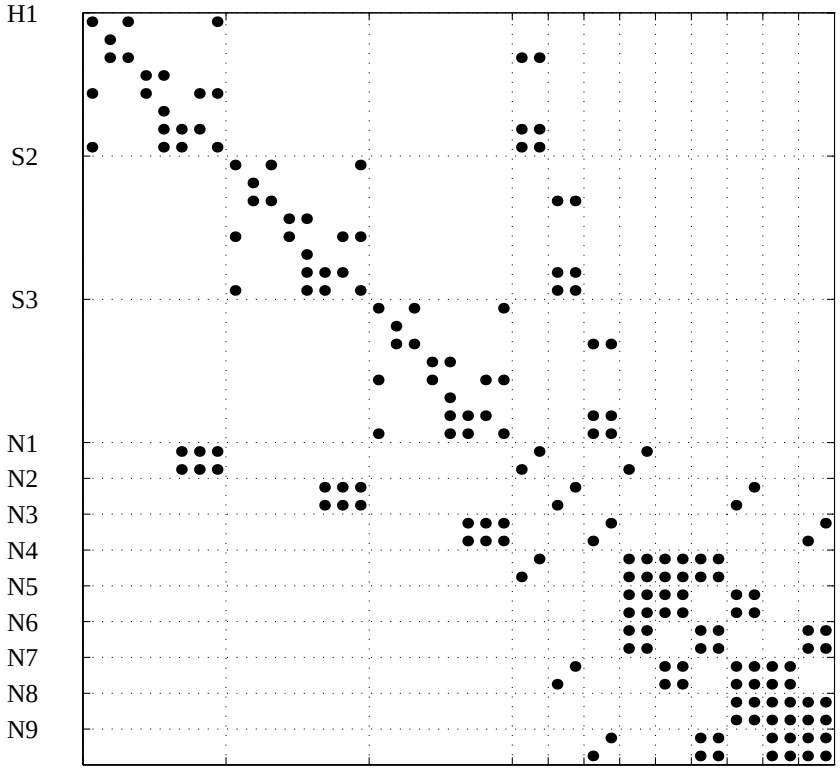

Fig. 2.6 Sparsity plot of the DAE system matrix A: dots represent nonzero elements and block matrices associated with the individual machines and buses are indicated.

Data of lines, transformers and machines are taken from [Anderson and Fouad 1993], while models of AVR and governor are described in Appendix B. The normal load situation in Fig. 2.5 from [Anderson and Fouad 1993] gives an operating point with one electro-mechanical mode at 1.3 Hz and one at 1.8 Hz. The machine angle elements of the corresponding right eigenvectors are given in Table 2.1.

Machine	1.3 Hz mode	1.8 Hz mode
H1	$0.277e^{-j4^\circ}$	$0.029e^{-j111^\circ}$
S2	$0.818e^{j179^\circ}$	$0.282e^{-j127^\circ}$
S3	$0.495e^{-j179^\circ}$	$0.948e^{j62^\circ}$

Table 2.1 Machine angle elements of the right eigenvectors corresponding to the oscillatory electro-mechanical modes.

If the arguments of the eigenvector elements are concentrated around two values that are separated by 180°, one of them may be used as reference and the angle information may be described as in-phase or anti-phase. This can be illustrated by a bar graph as in Fig. 2.7 and is known as the *mode shape*. It shows that all machines are active in the 1.3 Hz mode, while mainly S2 and S3 swing against each other during the 1.8 Hz mode.

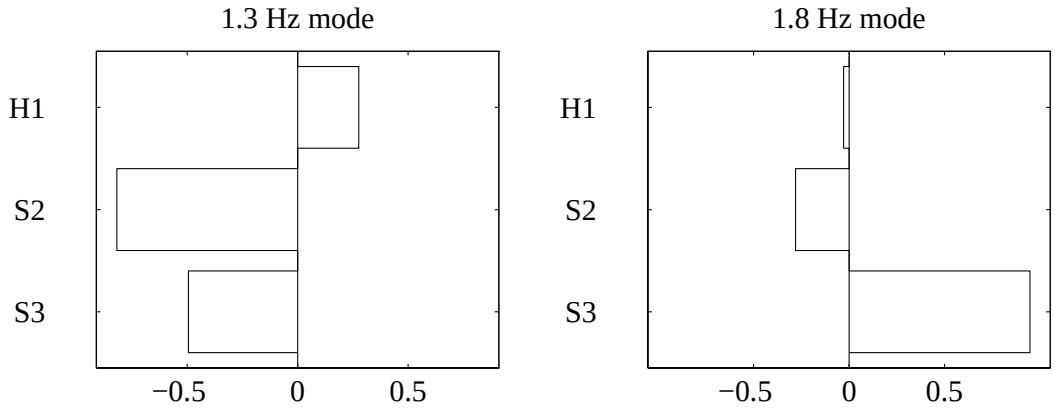

Fig. 2.7 Mode shape of the 1.3 Hz mode (left) and the 1.8 Hz mode (right).

Twenty-three Machine System

The twenty-three machine system is the *Nordic32* or *the Swedish test system* of the report *Long Term Dynamics Phase II* by CIGRÉ TF 38-02-08 [CIGRÉ 1995]. The report compares long term dynamics of five test systems using ten different simulation tools. Although being fictitious the Swedish test system has dynamic properties similar to the Swedish and Nordic power system. It is included here to illustrate what implications the studied damping schemes would have on a realistic system.

As can be seen in Fig. 2.8, the system is divided into three Swedish areas denoted Southwest, Central, North and and a foreign part named External. The external and northern regions are characterized by a large amount of hydro power generation, while the other two hold thermal power plants. The External and the Southwest areas are essentially self-supporting in contrast to the Central region, which imports half its power consumption from North.

The nineteen 400 kV transmission system buses in Fig. 2.8 are given four-digit node numbers starting with 4. Similarly the two 220 kV buses and the eleven 130 kV buses of the subtransmission system have numbers starting with 2 and 1 respectively. Nine pure load buses at 130 kV have two-digit numbers and are connected to the 400 kV network via transformers with tap changers. Out of the totally forty-one buses, twenty are generator buses,

holding twenty-three synchronous generators. Transformers are shown as lines that connect different voltage levels.

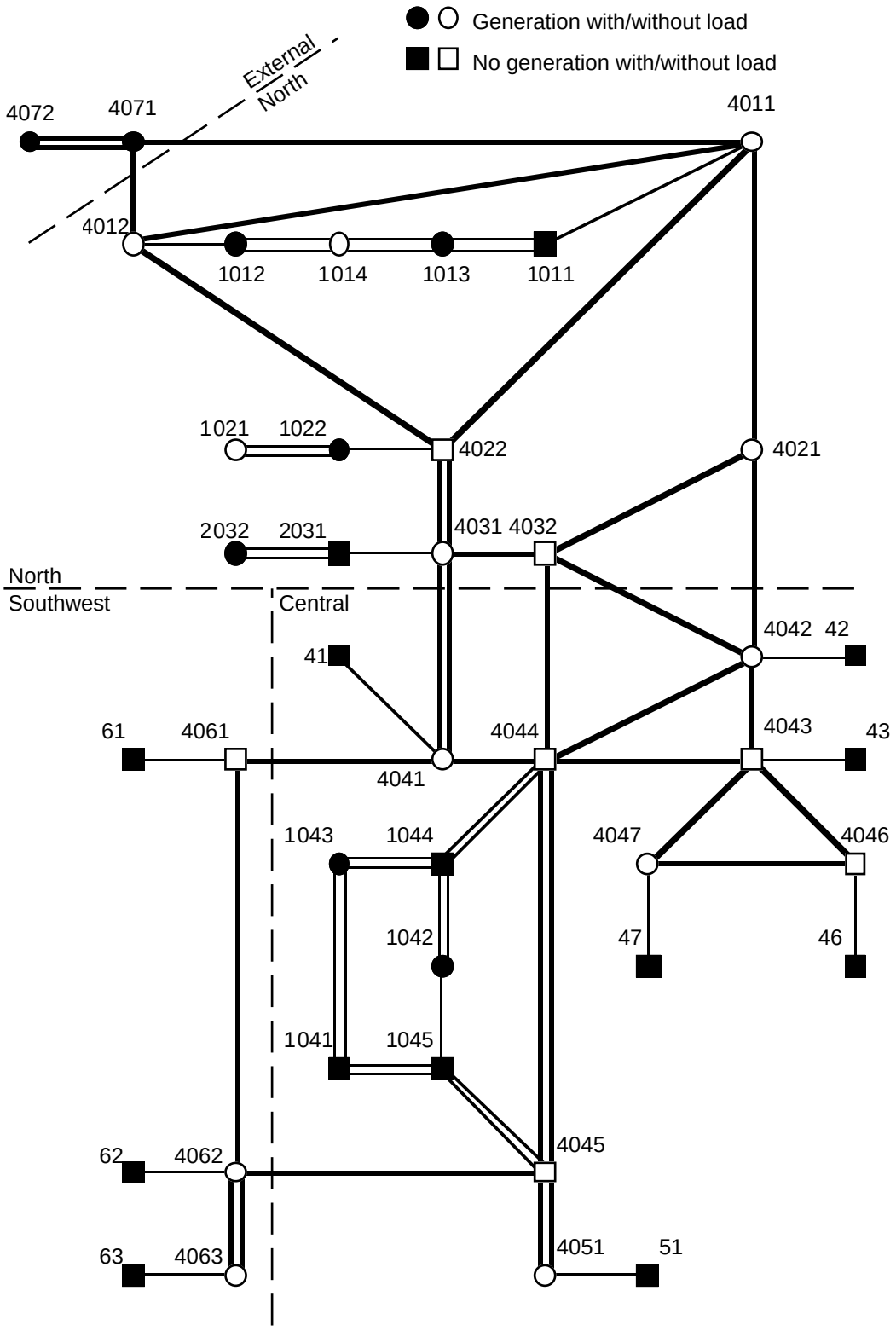

Fig. 2.8 Outline of the twenty-three machine system.

The EUROSTAG model of the twenty-three machine system has the very same structure as that of the three machine system. The main difference, except for the number of components, is that more detailed subsystem models are employed. This applies in particular for the machines and their controls, but also for loads and transformers. Although the test system is designed for simulations of transient stability and long term dynamics, the detailed modelling makes it suitable also for small disturbance stability analysis. The numerical data of the entire system is found in [CIGRÉ 1995] while the modifications that are used here are outlined in Appendix C. The model used in the following has 324 dynamic states and 221 algebraic states giving a total size of the *A* matrix of 545x545 elements.

As the machine model should reproduce transient behaviour, the fifth order model of EUROSTAG is chosen [EUROSTAG]. It includes damper windings in both the *d* and *q* axis as well as saturation modelling. The excitation system is modelled as a second order system. The AVR includes a Power System Stabilizer (PSS) with output limited to ± 5% and limiters for both stator and rotor currents. The current limits play a very important role when the system is close to voltage collapse, but are not needed when studying damping. While generators of thermal power plants operate with constant mechanical power, the generators of hydro power plants are equipped with governors and models of the water ways.

The machines can be divided into three groups: ten round rotor generators in thermal power stations (4042, 4047_1, 4047_2, 4051_1, 4051_2, 4062, 4063_1, 4063_2, 1042, 1043), twelve salient pole generators in hydro power stations (at buses 4011, 4012, 4021, 4031, 4071, 4072, 1012, 1013, 1014, 1021, 1022, 2032) and a salient pole synchronous compensator (at bus 4041). The machines have different ratings, but in each group all use the same set of parameters (in per unit of machine base) for the generator, the PSS and the governor.

In the CIGRÉ model, distribution networks are modelled as loads with voltage and frequency dependencies according to (2.28),

$$P_{load} = P_0 \left[\frac{V}{V_0} + \left(\frac{f}{f_0} \right)^{0.75} \right] \tag{2.28a}$$

$$Q_{load} = Q_0 \left(\frac{V}{V_0} \right)^2 \tag{2.28b}$$

The voltage dependence of loads is critical when studying voltage collapse or damping by PSS or SVC, as these are voltage related phenomena. A realistic improvement of the distribution systems modelling would be to incorporate dynamic voltage dependence as in [Karlsson and Hill 1994].

Detailed transformer models with tap changer control are used for the nine load transformers and for the four transformers connecting the 130 kV area to nodes 4044 and 4045. The remaining four transformers, all in the area North, have fixed ratios. Tap changer action and load dynamics are both very important for the load restoration, that is an important cause of voltage collapse. For small disturbance stability studies, however, neither is usually considered. But as the tap changers are already included they are retained for convenience.

The three scenarios proposed in [CIGRÉ 1995] are all designed to cause a voltage collapse, similar to that of the Swedish black-out in 1983 [Kearsley 1987]. In all three cases a generation unit is tripped, in one case after the tripping of the important transmission line between 4011 and 4021. The resulting new load flow situation causes generator current limiters to act and subsequently the tap changers operate to restore the voltage. As the load increases faster than the voltage, a voltage collapse occurs.

Tripping of a generator is a large disturbance. A new scenario is therefore required for small disturbance stability studies. [CIGRÉ 1995] suggests two load flow cases characterized as peak load and high load. The high load case for the intact network is used as base case. The damping controller to be designed should manage different operating points. Disconnecting a transmission line substantially changes the load flow. It can also change the swing mode pattern of the generators, which is seen in the eigenvectors of the linearized system. The double line between 4044 and 4045 is found to have this influence, and although unlikely its tripping is not unrealistic.

In order to obtain a reasonable voltage profile for the fault case with line 4044-4045 out, a few changes are necessary. Generator buses were previously modelled as PQ buses making all AVRs passive. This is improved by instead using PV buses. The voltage setpoints are taken from the base case, but are adjusted so that the reactive generation limits that are unaltered, are not activated in either case.

All modes are well damped, which is mainly due to the fact that PSS units with perfectly matching parameters are installed on all generators. To worsen the situation, the PSSs of the generators at all thermal power plants were disengaged. This is not unrealistic and reduces the damping of modes

where machines in the Central and Southwest participate. This use of PSS is the same in the base case and the fault case, where the line N4044-N4045 is disconnected.

The control system design will aim at improving damping of the least damped modes in the fault case and therefore the three modes of Table 2.2 have been chosen for closer study.

Mode	Base case	Fault case
1	-0.14±j3.38	-0.09±j3.09
2	-0.36±j5.74	-0.21±j4.47
3	-0.31±j4.62	-0.22±j4.64

Table 2.2 Eigenvalues of the selected modes in the base case and in the fault case.

Note that the fault substantially changes the frequency of Mode 2, which is the reason for numbering the modes rather than naming them by their frequency. The modes are instead identified by their mode shape shown in Fig. 2.9a. The geographical shape of the mode is shown in the network diagram of Fig. 2.9b, where the absence of the transmission line N4044-N4045 in the fault case is apparent. Whereas Mode 1 has nearly identical shape in both cases, Mode 2 and 3 are identified as follows: Mode 2 is an oscillation between the machines on each side of the disconnected line, and is therefore expected to change radically. Mode 3 is a swing mode between two groups, where N4051 is close to the disconnected line and changes side due to the fault.

It is evident that both frequency, damping and structure of the mode is altered by the fault. As a damping system should be able to handle such changes, the chosen fault is a suitable challenge.

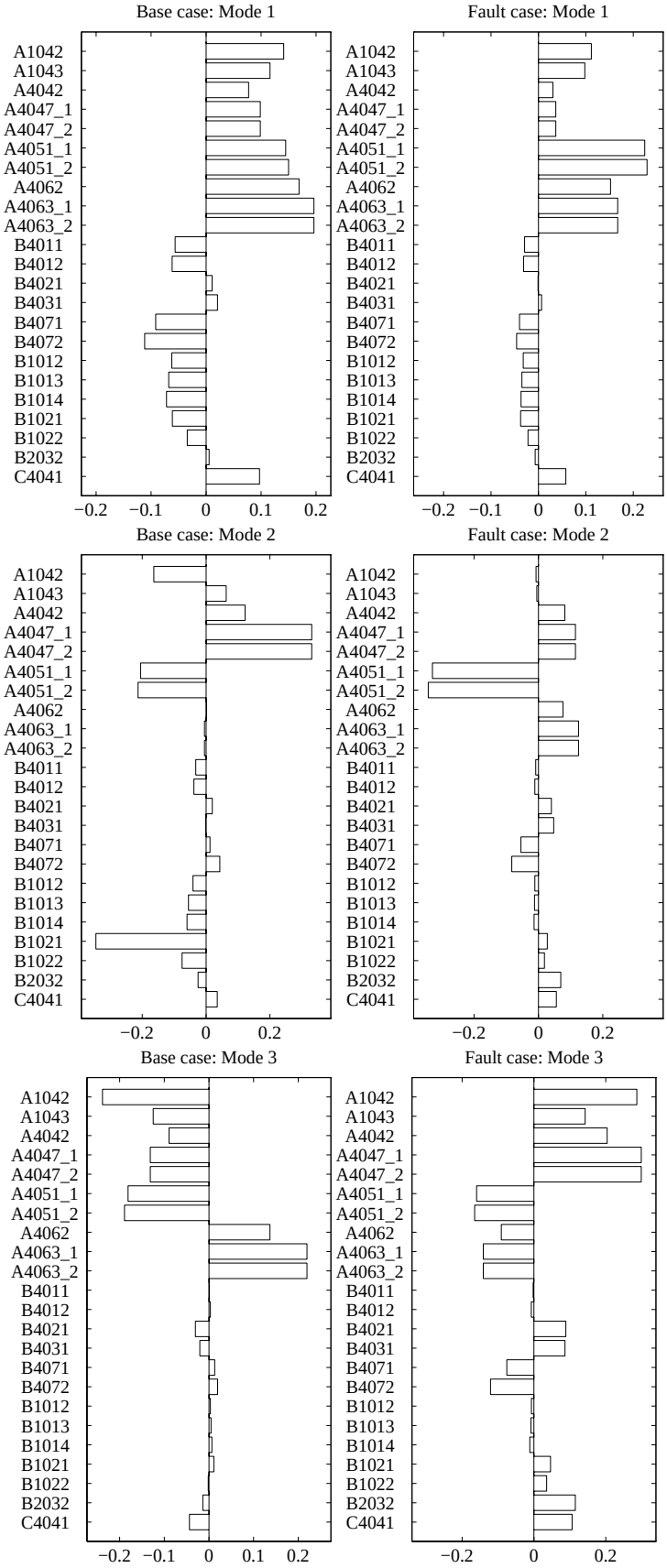

Fig. 2.9 a Mode shapes of the study modes for base case (left) and fault case (right).

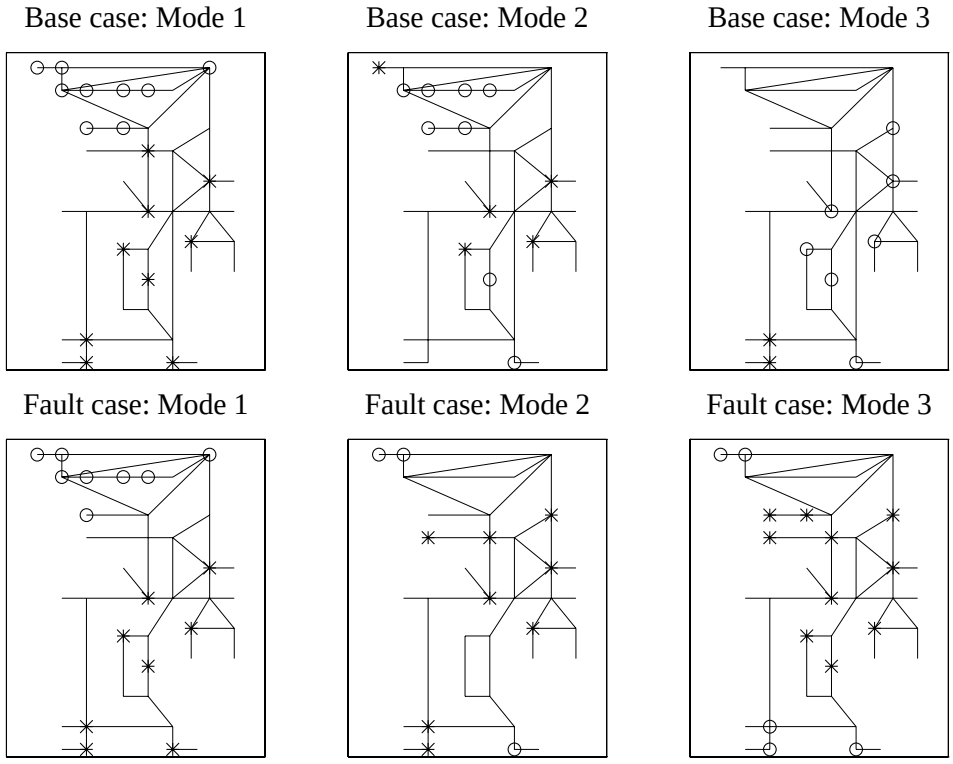

Fig. 2.9 b Swing patterns of the study modes for the base case (upper graphs) and the fault case (lower graphs). The two swing directions are illustrated by '*' and 'o' respectively. Machines with less than 10 % of the peak amplitude are not included.

2.4 Mechanical Equivalents

To gain insight into the behaviour of complex systems, the existence of a well understood analogy is often useful. Electromechanical dynamics of power systems can for example be transformed into purely electrical or mechanical systems. Mechanical equivalents are for example employed in [Elgerd 1971] and [Kimbark 1948]. Animation of power system dynamics using a mechanical equivalent is described in [Gronquist et al 1996]. The models described in the following are used throughout the thesis to provide a more intuitive insight into the power system dynamics.

Spring-Mass Model of an Inter-Area Mode

Fig. 2.10 shows a spring-mass model, that exhibits the dynamics of the inter-area mode mentioned in Section 2.2.

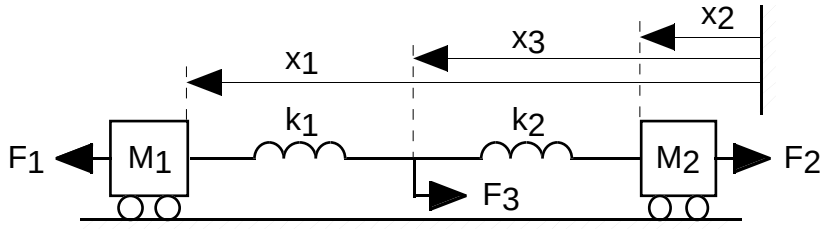

Fig. 2.10 Spring-mass model of an inter-area mode.

The masses M_1 and M_2, with positions x_1 and x_2, symbolize the machine groups that swing against each other. F_1 and F_2 is the *constant* mechanical power input of each equivalent machine. Transmission lines are represented by two springs with constants k_1 and k_2. A force F_3, corresponding to controlled active power, acts on the node with position x_3 between the springs. Force balances at positions x_1, x_2 and x_3 give,

$$\begin{aligned} M_1\ddot{x}_1 &= k_1(x_3 - x_1) + F_1 \\ M_2\ddot{x}_2 &= k_2(x_3 - x_2) - F_2 \\ 0 &= k_1(x_1 - x_3) + k_2(x_2 - x_3) - F_3 \end{aligned}$$

A DAE matrix model may now be formulated by introducing the states v_1 and v_2 as horizontal velocities of the two masses,

$$diag\left(\begin{bmatrix} M_1 \\ M_2 \\ 1 \\ 1 \\ 0 \end{bmatrix}\right)\frac{d}{dt}\begin{bmatrix} v_1 \\ v_2 \\ x_1 \\ x_2 \\ x_3 \end{bmatrix} = \left[\begin{array}{cccc|c} 0 & 0 & -k_1 & 0 & k_1 \\ 0 & 0 & 0 & -k_2 & k_2 \\ 1 & 0 & 0 & 0 & 0 \\ 0 & 1 & 0 & 0 & 0 \\ \hline 0 & 0 & k_1 & k_2 & -(k_1+k_2) \end{array}\right]\begin{bmatrix} v_1 \\ v_2 \\ x_1 \\ x_2 \\ x_3 \end{bmatrix} + \begin{bmatrix} 1 & 0 & 0 \\ 0 & -1 & 0 \\ 0 & 0 & 0 \\ 0 & 0 & 0 \\ 0 & 0 & -1 \end{bmatrix}\begin{bmatrix} F_1 \\ F_2 \\ F_3 \end{bmatrix} \quad (2.29)$$

By creating block matrices as indicated by the lines above, the model structure becomes apparent,

$$diag\left(\begin{bmatrix} M \\ I \\ 0 \end{bmatrix}\right)\frac{d}{dt}\begin{bmatrix} v \\ x_d \\ x_a \end{bmatrix} = \left[\begin{array}{cc|c} 0 & K_{dd} & K_{da} \\ I & 0 & 0 \\ \hline 0 & K_{ad} & K_{aa} \end{array}\right]\begin{bmatrix} v \\ x_d \\ x_a \end{bmatrix} + \begin{bmatrix} K_{du} \\ 0 \\ K_{au} \end{bmatrix}F$$

This generalization is valid for any configuration of masses and springs. Note that the same statement, but for a power system, was made for the power system model of (2.22), that has the same structure. The agreement between the electro-mechanical model and its mechanical equivalent is thus demonstrated.

The system of (2.29) has four eigenvalues,

$$\begin{aligned}\lambda_1 &= \lambda_2^* = j\sqrt{\frac{k_1 k_2}{k_1 + k_2}\left(\frac{1}{M_1} + \frac{1}{M_2}\right)} \\ \lambda_3 &= \lambda_4 = 0\end{aligned} \tag{2.30}$$

where the first two are oscillatory and form the equivalent to the electro-mechanical inter-area mode, whereas the last two form a *rigid body mode*. The right and left eigenvectors of the oscillatory mode are,

$$\begin{aligned}\Phi_1 &= \Phi_2^* = \begin{bmatrix} \frac{\lambda_1}{M_1} & \frac{-\lambda_1}{M_2} & \frac{1}{M_1} & \frac{-1}{M_2} \end{bmatrix}^T \\ \Psi_1 &= \Psi_2^* = \begin{bmatrix} \frac{1}{\lambda_1} & \frac{-1}{\lambda_1} & 1 & -1 \end{bmatrix} \kappa\end{aligned} \tag{2.31}$$

where

$$\kappa = \frac{M_1 M_2}{2\left(M_1 + M_2\right)}$$

is introduced so that $\Phi_1\Psi_1$=1. The right and left eigenvectors of the rigid body mode are,

$$\begin{aligned}\Phi_3 &= -\Phi_4 = \begin{bmatrix} 0 & 0 & 1 & 1 \end{bmatrix}^T \\ \Psi_3 &= -\Psi_4 = \begin{bmatrix} \frac{1}{M_2} & \frac{1}{M_1} & 0 & 0 \end{bmatrix}\end{aligned} \tag{2.32}$$

Φ_3 and Φ_4 describe a motion where the entire system, with masses and springs, slide in either direction as a *rigid body*. This term is used in power system contexts to describe a uniform motion of all synchronous machine rotor angles. In a power system one of the zero eigenvalues moves away from the origin if damping relative to fixed frequency is introduced. The other is usually eliminated by appointing one bus as reference, to which all angles are related. This reduces the length of the state vector by one element.

Spring-Mass Model of a Local Mode

The mechanical equivalent of the single machine infinite bus system can be obtained from the system above. M_2 is then turned into a fixed reference –

the infinite bus – by setting $M_2=\infty$ and fixing its position to zero. The rows and columns corresponding to v_2 and x_2 can be removed together with the states themselves as x_3 is renamed to x_2,

$$\begin{bmatrix} M_1 & & \\ & 1 & \\ & & 0 \end{bmatrix} \frac{d}{dt} \begin{bmatrix} v_1 \\ x_1 \\ x_2 \end{bmatrix} = \begin{bmatrix} 0 & -k_1 & k_1 \\ 1 & 0 & 0 \\ 0 & k_1 & -(k_1+k_2) \end{bmatrix} \begin{bmatrix} v_1 \\ x_1 \\ x_2 \end{bmatrix} + \begin{bmatrix} 1 & 0 \\ 0 & 0 \\ 0 & -1 \end{bmatrix} \begin{bmatrix} F_1 \\ F_2 \end{bmatrix} \quad (2.33)$$

Equation (2.33) describes the system of Fig. 2.10 and is equivalent to (2.20), previously mentioned.

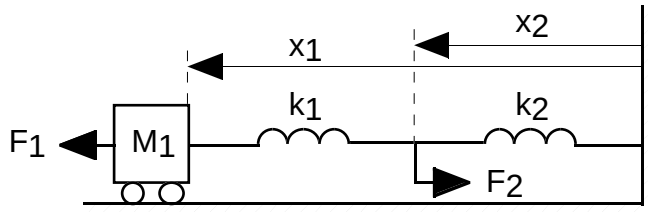

Fig. 2.11 Spring-mass model of the single machine infinite bus system.

This system has one complex conjugate pair of eigenvalues,

$$\lambda_1 = \lambda_2^* = j\sqrt{\frac{k_1 k_2}{k_1+k_2}\frac{1}{M_1}}$$

which could have been obtained by setting M_2 in λ_1 and λ_2 of the two-mass system to infinity. The right and left eigenvectors of this mode are,

$$\Phi_1 = \Phi_2^* = \begin{bmatrix} \lambda_1 & 1 \end{bmatrix}^T$$

$$\Psi_1 = \Psi_2^* = \begin{bmatrix} \frac{1}{2\lambda_1} & \frac{1}{2} \end{bmatrix}$$

Pendulum Equivalent to Local Mode

The spring-mass models above are naturally not the only mechanical systems, that can be constructed as dynamic equivalents to power systems. Fig. 2.12 shows the single machine system of 2.3 and a mechanical pendulum equivalent that also exhibits visual similarities.

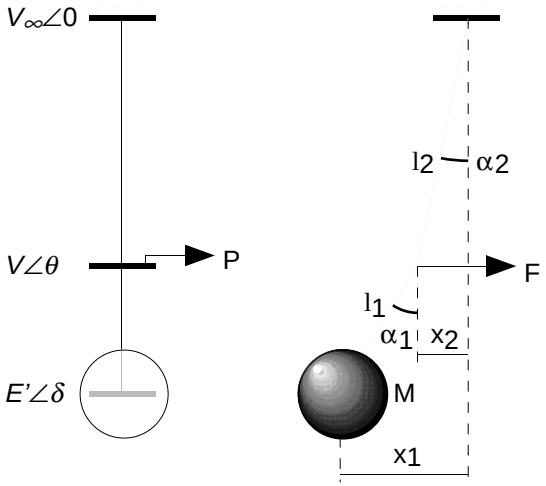

Fig. 2.12 Single machine system and a mechanical equivalent.

The pendulum is vertical and consists of a mass suspended in a massless, but flexible string. The active load P of the power system is represented by a force F acting on the string. The deflections x_1 and x_2 from the stationary point correspond to the phase angles δ and θ. By assuming that x_1 and x_2 are small a linear model can be formulated. Let the force along the lower and upper part of string be F_1 and F_2 respectively. Vertical force balances at the mass center and the attack point of F yield (2.34), that applies for small angles α_1 and α_2,

$$\begin{aligned} F_1 \cos\alpha_1 &= Mg \\ F_2 \cos\alpha_2 &= F_1 \cos\alpha_1 \end{aligned} \Rightarrow F_1 \approx F_2 \approx Mg \tag{2.34}$$

Horizontal force balances at the same points give,.

$$\begin{aligned} M\left(l_1\ddot{\alpha}_1 + l_2\ddot{\alpha}_2\right) &= -F_1 \sin\alpha_1 \\ F_1 \sin\alpha_1 &= F_2 \sin\alpha_2 + F \end{aligned} \tag{2.35}$$

F_1 and F_2 are eliminated and the equations are linearized, leading to

$$\begin{aligned} l_1\ddot{\alpha}_1 + l_2\ddot{\alpha}_2 &= -g\alpha_1 \\ \frac{1}{M}F &= g\left(\alpha_1 - \alpha_2\right) \end{aligned} \tag{2.36}$$

α_1 and α_2 are now replaced by x_1 and x_2 through the transformation,

$$\begin{cases} x_1 = l_1\alpha_1 + l_2\alpha_2 \\ x_2 = l_2\alpha_2 \end{cases} \Leftrightarrow \begin{cases} \alpha_1 = \dfrac{1}{l_1}(x_1 - x_2) \\ \alpha_1 - \alpha_2 = \dfrac{1}{l_1}x_1 - \left(\dfrac{1}{l_1} + \dfrac{1}{l_2}\right)x_2 \end{cases}$$

By introducing v_1 as the velocity of x_1 the DAE system description is complete,

$$\begin{bmatrix} 1 & & \\ & 1 & \\ & & 0 \end{bmatrix} \frac{d}{dt} \begin{bmatrix} v_1 \\ x_1 \\ x_2 \end{bmatrix} = \begin{bmatrix} 0 & -\dfrac{g}{l_1} & \dfrac{g}{l_1} \\ 1 & 0 & 0 \\ 0 & \dfrac{g}{l_1} & -g\left(\dfrac{1}{l_1} + \dfrac{1}{l_2}\right) \end{bmatrix} \begin{bmatrix} v_1 \\ x_1 \\ x_2 \end{bmatrix} + \begin{bmatrix} 0 \\ 0 \\ -\dfrac{1}{M} \end{bmatrix} F \qquad (2.37)$$

The eigenvalues of this system are,

$$\lambda_1 = \lambda_2^* = j\sqrt{\frac{g}{l_1 + l_2}}$$

and the corresponding right and left eigenvectors are,

$$\Phi_1 = \Phi_2^* = \begin{bmatrix} \lambda_1 & 1 \end{bmatrix}^T$$

$$\Psi_1 = \Psi_2^* = \begin{bmatrix} \dfrac{1}{2\lambda_1} & \dfrac{1}{2} \end{bmatrix}$$

It is evident that the pendulum as described by (2.37) is equivalent both to the spring-mass model of (2.33) and to the single machine infinite bus system of (2.20). It is therefore natural, that both eigenvalues and eigenvectors look like those of the other local mode system.